Available online at www.sciencedirect.com
ScienceDirect
Journal of Power Sources 165 (2007) 114–119
JOURNAL OF POWER SOURCES
www.elsevier.com/locate/jpowsour

Short communication

Electrochemical impedance investigation of the redox behaviour of a Ni–YSZ anode

Bin Liu [a,b], Yun Zhang [a,b], Baofeng Tu [a,b], Yonglai Dong [a], Mojie Cheng [a,*]

[a] *Dalian Institute of Chemical Physics, Chinese Academy of Sciences, Dalian 116023, China*
[b] *Graduate University of the Chinese Academy of Sciences, Beijing, China*

Received 23 October 2006; received in revised form 27 November 2006; accepted 27 November 2006
Available online 18 January 2007

Abstract

The reoxidation and reduction of a Ni–YSZ anode were investigated by monitoring the variation of ohmic resistance and the open circuit voltage of anode supported cells using electrochemical impedance spectroscopy. The ohmic resistance curves showed that anode reoxidation could be largely divided into three stages: an initial stage with a slow increase of ohmic resistance, a quick oxidation stage with a sharp increase in ohmic resistance and a final stage with a slight decrease of ohmic resistance. Reoxidation at 800 °C was a rapid process with a short initial stage, whereas reoxidation at 500 °C did not proceed in the last two stages. The OCV curves showed that reoxidation above 600 °C caused cracking of the YSZ electrolyte film.

Keywords: Ni–YSZ anode; Ohmic resistance; Reoxidation; Reduction; NiO

1. Introduction

Solid oxide fuel cells (SOFCs) are a promising new technology for highly efficient, environmental-friendly power generation. The anode-supported design is by far the most widely employed in state-of-the-art SOFCs due to its higher power density and lower fabrication cost [1–4]. In a typical anode supported cell, the anode is a porous Ni–YSZ cermet with a thickness between 0.5 and 2 mm. The electrolyte is a thin (∼10 μm) and dense YSZ layer supported on the anode substrate. The cathode is usually a porous composite of strontium-doped manganite ($La_{1-x}Sr_xMnO_{3-\delta}$, LSM) and YSZ electrolyte.

With rapid progress in power density and cost reduction, the stabilities, including both the thermal-cycling stability and redox stability, become one of most important issues from various practical considerations. In a real SOFC system, cyclic reduction and oxidation (redox) can unavoidably occur for various reasons, such as the occasionally break-down of the fuel supply at the operating temperature or failure in cell sealing. The redox behaviour of nickel will result in large bulk volume changes, which may have a detrimental effect on the electrolyte film, anode microstructure and the integrity of the anode/electrolyte interfaces, and lead to performance degradation or cell failure.

The volume change of nickel during the reduction of a sintered NiO–YSZ does not appear to damage the electrolyte, but the reoxidation of nickel might lead to the cracking of electrolyte [5]. Reoxidation could lead to an increase of polarization resistance, which is ascribed to the formation of cracks within the anode [6]. Waldbillig et al. have observed that the amount of cracks was reduced by lowering the Ni content in the anode and by reducing the reoxidation temperature. The cell performance degradation after redox at 750 °C has also been observed [7,8]. Malzbender et al. have revealed that after reoxidation, nickel oxide particles have a higher porosity and the anode expansion causes tensile stresses to develop in the electrolyte, ultimately causing fracture [9].

Up to now, most researches on the anode redox behaviour have been carried out either on the Ni–YSZ cermet during the redox process or on the cell after the redox process, which showed the historical effects of the redox process of a Ni–YSZ cermet and the cell degradation. An important need for understanding the redox behaviour is in situ monitoring and analysis of the practical changes in a cell during the redox process. In

* Corresponding author. Tel.: +86 411 84379049; fax: +86 411 84379049.
E-mail address: mjcheng@dicp.ac.cn (M. Cheng).

0378-7753/$ – see front matter © 2006 Elsevier B.V. All rights reserved.
doi:10.1016/j.jpowsour.2006.11.052

this study, the redox process of an anode-supported cell was followed by the measurements of ohmic resistance and open circuit voltage using electrochemical impedance spectroscopy (EIS).

2. Experimental

2.1. Cell preparation

All the cells used in this work were batch-prepared using a two-step co-firing method. Firstly, commercial 8 mol% yttria stabilized zirconia (YSZ, Tosoh Corporation) and nickel oxide (NiO, J.T. Baker Corporation) powders were mixed in the proportion of 50:50 (wt%) with solvent and organic binders, and then tape-cast into an anode substrate. The YSZ electrolyte was slurry-coated on the green substrate and then cut into individual discs of 2 cm in diameter. These electrolyte–anode bilayered discs were fired at 1400 °C. A $La_{0.50}Sr_{0.50}MnO_3$ (LSM)/YSZ composite cathode was applied onto the electrolyte film by screen-printing method and fired at 1200 °C for 2 h. The anode thickness was ca. 800 μm, and the electrolyte thickness was ca. 10 μm. The cathode was ca. 0.50 cm^2 in area and ca. 50 μm in thickness. All the cells had the same structure and compositions. The weight error between cells was less than 2%.

2.2. Course of anode redox

The cells were tested in an apparatus, as shown in Fig. 1. The cell was sandwiched between two alumina tubes. Silver mesh, which was spring-pressed onto the anode and cathode sides, was used as both current collectors. The cathode side was sealed with a flexible gasket. The anode side was sealed with a glass ring. To assure gas tightness, the anode side seal was checked with a nitrogen flow at 800 °C before anode reduction. With successful sealing, bubbles in water from the anode outlet could be observed with a 0.5 ml min^{-1} nitrogen flow. Through the experiments, the flowing rate of O_2 to the cathode chamber was maintained at 50 ml min^{-1}.

The redox of anode was performed as below. First, all the sintered anodes were reduced at 800 °C with a 5% H_2 and 95% He blending gas at 100 ml min^{-1}. Then, the anodes were reoxidized under a flow of 50 ml min^{-1} air at 500, 600, 700 and 800 °C, respectively. Finally, the anodes were reduced again with 5% H_2 and 95% He at 100 ml min^{-1} and at 500, 600, 700 and 800 °C, respectively. During the experiments, highly pure helium was flowed for 10 min between atmosphere changes. All the gases were introduced to the anode through a water bubbler at room temperature.

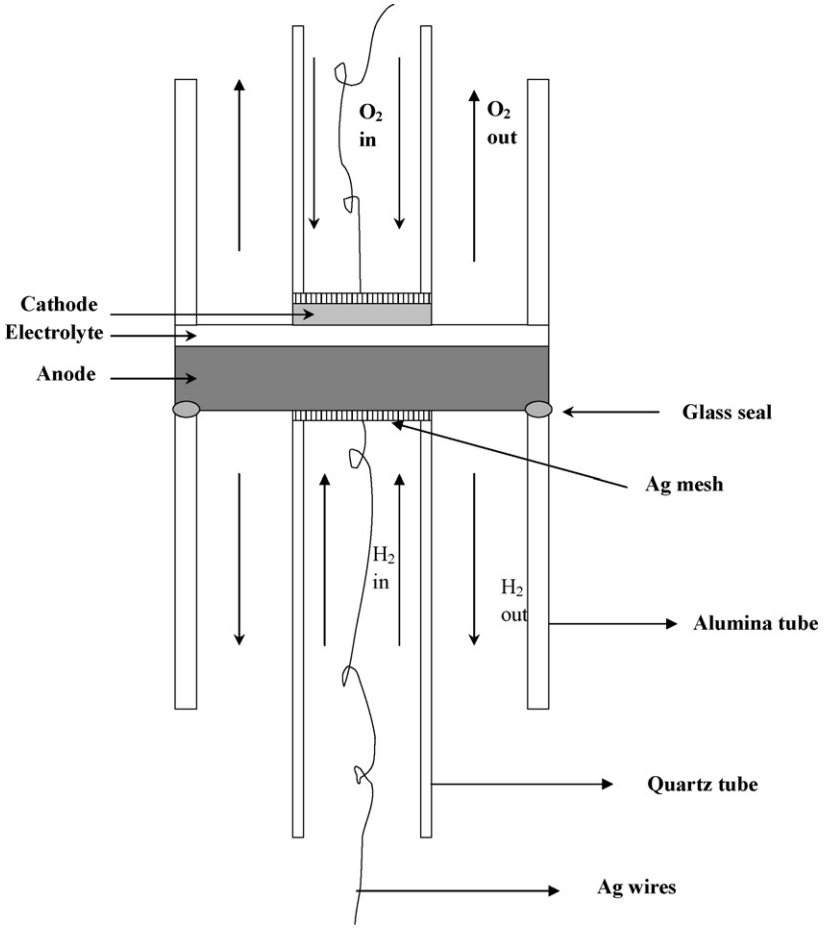

Fig. 1. Schematic of the cell testing apparatus.

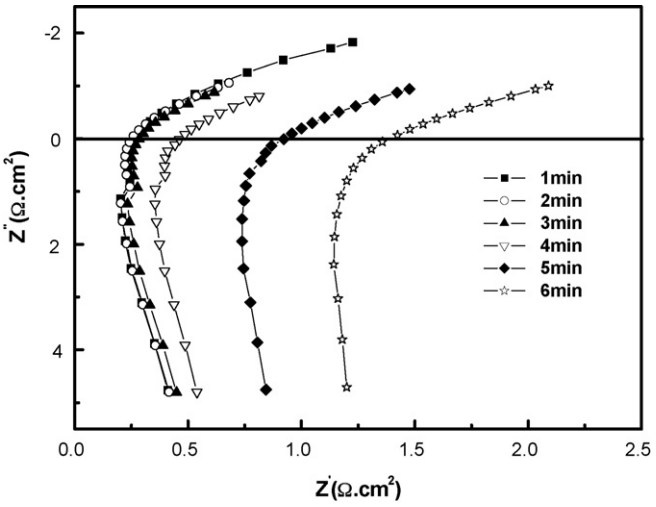

Fig. 2. Nyquist plots showing the variation of cell ohmic resistance with anode reoxidation at 800 °C.

2.3. Monitoring of by EIS

The impedance of the cells was measured typically by the two electrode method under open circuit conditions using a Solartron 1287 potentiostat and 1260 frequency response analyzer combined with a computer. The measurement was used to record the ohmic resistance and open circuit voltage. In order to follow the fast reoxidation and reduction process, the impedance spectra in the frequency range from 10^6 to 9000 Hz were taken with a signal amplitude of 10 mV. One impedance spectrum was recorded each minute.

In a Nyquist plot, the real axis Z' represents the resistance value with sweeping frequency and the imaginary axis Z'' represents the capacitance (the first quadrant) or inductance (the fourth quadrant). The intercept of the impedance spectrum with the Z'-axis in the high-frequency range is usually considered to be the total ohmic resistance, which is the sum of anode ohmic resistance, cathode ohmic resistance, electrolyte resistance and contact and lead resistance.

Fig. 2 gives some examples of EIS with anode reoxidation time at 800 °C. The ohmic resistance changed little in the initial 3 min, but began to increase dramatically after the fourth minute. The corresponding ohmic resistance plot with time might give us some information about anode during redox. The conversion of Ni and NiO during reduction or NiO to Ni during oxidation will cause a large difference in electrical conductivities, and the variation of the anodic ohmic resistance can be expected. The ohmic resistance for a 20 μm-thick YSZ film is only 0.05 Ω cm^2 at 800 °C, and it is about 5 Ω cm^2 at 500 °C [10]. The ohmic resistance for the cathode is a result from the resistances of LSM, YSZ and silver paste for current collecting. The resistance of silver is much smaller than the other two, and it will vary little with anode redox changes. The contact and lead resistance will not change with the redox because a spring-pressed structure was used for current collecting. Therefore, the change of the total cell resistance will mainly come from the anode during redox changes.

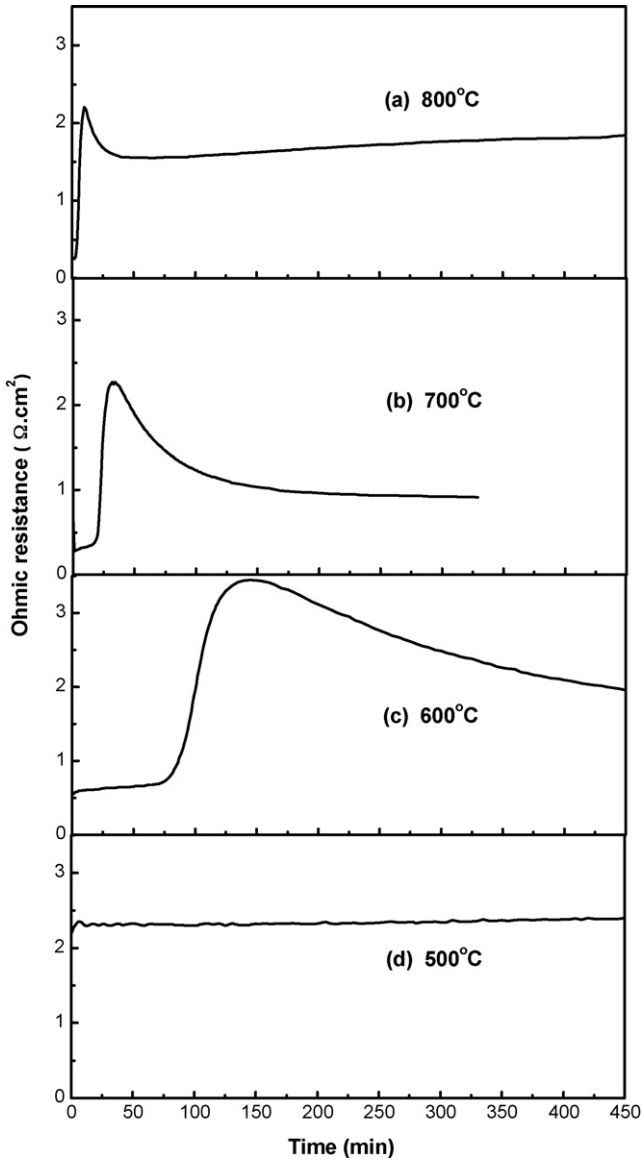

Fig. 3. Variation of the cell ohmic resistance with anode reoxidation time at (a) 800 °C, (b) 700 °C, (c) 600 °C and (d) 500 °C.

3. Results and discussion

3.1. Reoxidation of Ni–YSZ anodes

After the sintered anodes were reduced at 800 °C, the Ni–YSZ anodes were exposed to flowing air at 500, 600, 700 and 800 °C, respectively. Fig. 3 shows the variation of ohmic resistance with reoxidation time. Similar ohmic resistance curves are shown for the reoxidation at 600, 700 and 800 °C. Based on the ohmic resistance change, the anode reoxidation can largely be divided into three stages, including an initial stage with a slow increase of ohmic resistance, a quick oxidation stage with a sharp increase of ohmic resistance and the last stage with a slight decrease of ohmic resistance. In the initial oxidation stage, the ohmic resistance increases very slowly, suggesting that oxidation might occur on the surfaces of nickel particles without a significant impact on the Ni–Ni electronic conduction network. The second

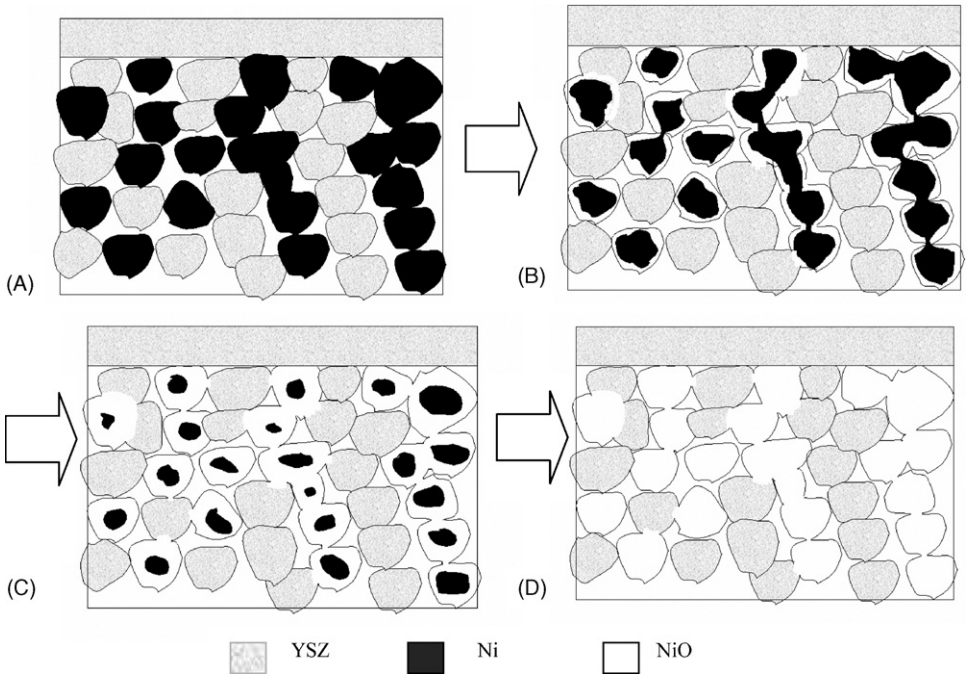

Fig. 4. Schematic illustration on the different oxidation stages: (A) anode with nickel conduction network before reoxidation, (B) anode in the initial reoxidation stage, (C) anode in the rapid oxidation stage, and (D) NiO conduction network after complete reoxidation.

stage is featured with a sharp increase of ohmic resistance. In this stage, the inter-particle connections of nickel could be rapidly broken down with oxidation and at the end of this stage, the nickel electrical conduction network is completely destroyed. In the last stage, the ohmic resistance decreases with the oxidation process, suggesting the formation of a new conduction network from interconnections of NiO particles. The cell ohmic resistance at 500 °C is ca. 2.3 Ω cm^2, which is mainly from the resistance of the YSZ electrolyte film. Upon exposing to air, the total cell resistance remains unchanged, suggesting that reoxidation affect little on both the conductivity of anode and electrolyte. Our previous research showed that the conversion of Ni to NiO was ca. 10% under a pure oxygen atmosphere at 400 °C [11]. The incomplete oxidation of nickel affords the little variation in the ohmic resistance.

In a Ni–YSZ anode, the electrical conductivity is mainly determined by the nickel continuity [12,13]. The change of ohmic resistance with anode reoxidation can be illustrated by the schematic in Fig. 4. At the initial reoxidation stage, oxygen reacts with the surface layers of Ni and results in oxide scales, which were observed by Klemensø et al. [14]. Then, the NiO conducting network begins to form gradually. The oxidation at 500 °C might stop at this period with the formation of oxide scale. Anode conductivity is still dominated by the nickel network conductivity at this stage. With further oxidation, the nickel conduction network begins to be broken down. Both NiO and YSZ have a very low conductivity, which are several orders of magnitude lower than that of nickel. The ohmic resistance from anode dramatically increases at this period. The conversion of Ni to NiO would lead to the formation of large and porous nickel oxide particles. In theory, the bulk volume of a fully dense NiO sample should expand by 69.2% upon oxidation. The NiO particles from reoxidation have a sponge-like structure with higher porosity than the dense NiO particles in the sintered anode [8,9]. This results in a high conductivity of the NiO conducting network. On the hand, some cracks might generate on the YSZ film. The deposition of highly conductive materials such as silver in these cracks would also lead to a decrease in the total ohmic resistance. So, the decline of ohmic resistance would come from both nickel oxide and the deposits in these film cracks.

The rate-determining step for reoxidation in the porous Ni/YSZ cermet is nickel diffusion through the growing nickel oxide layer. Higher temperatures facilitate nickel diffusion and the conversion of Ni to NiO. The critical time when the total ohmic resistance attains the maximum value is 73, 19 and 3 min at 600, 700 and 800 °C, respectively. The shorter critical time for the reoxidation at higher temperature is reasonable. For the cell reoxidized at 500 °C, the ohmic resistance has little change up to 450 min, which indicates that the reoxidation rate is so slow that the nickel conduction network can not be destroyed.

3.2. Variation of open circuit potential during reoxidation

Fig. 5 shows the variation of the open circuit potential with oxidation time. The open circuit potential rapidly decreases after the introduction of air, indicating that the oxygen partial pressure in anode rapidly increases.

The theoretical open circuit potential at different conditions can be calculated by using Nernst equation:

$$E = \frac{RT}{4F} \ln \left(\frac{P_{O_{2(\text{cathode})}}}{P_{O_{2(\text{anode})}}} \right) \quad (1)$$

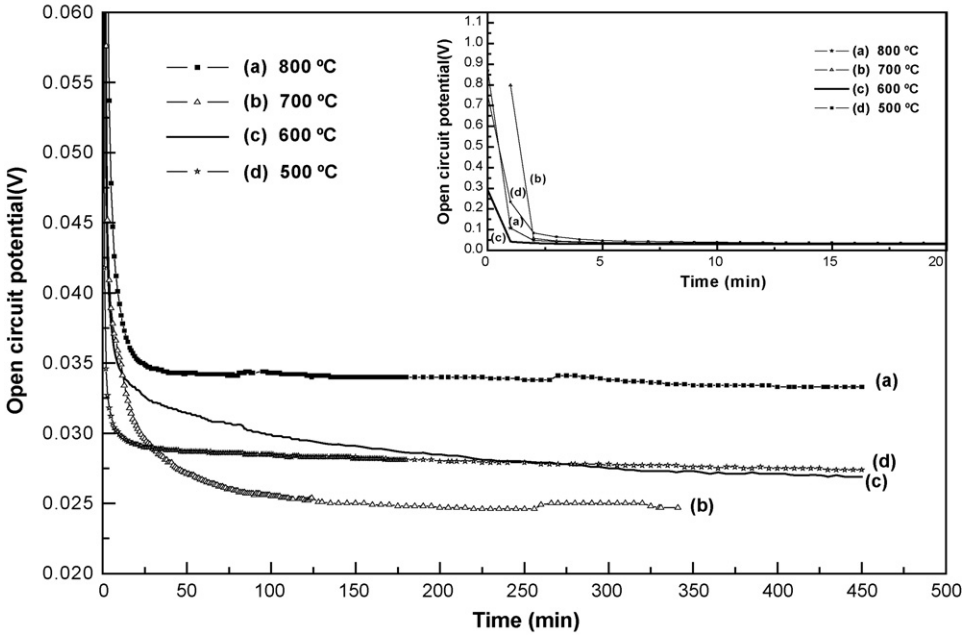

Fig. 5. Variation of open circuit potential with reoxidation time at (a) 800 °C, (b) 700 °C, (c) 600 °C and (d) 500 °C.

where E is the open circuit potential (V), R is the universal gas constant (8.314 J mol^{-1} K^{-1}), T is the temperature (K), F is the Faradic constant (96,485 C mol^{-1}), $P_{O_{2(anode)}}$ is the anodic oxygen partial pressure, and $P_{O_{2(cathode)}}$ is the oxygen partial pressure on the cathode side, which is 1 atm in our experiments.

At the end of reoxidation, the open circuit voltage (OCV) for the cell at 500 °C is 0.0274 V, which is very close to the theoretical value of 0.0268 V, indicating that the YSZ electrolyte film has withstood the reoxidation. This is consistent with the result from the ohmic resistance curve. The OCV for the cells reoxidized at 600, 700 and 800 °C is 0.0269, 0.0233, and 0.0338 V, respectively, which is far less than the corresponded theoretical values of 0.0303, 0.0337 and 0.0372 V. Thus, the OCV results also depict that the cells reoxidized at above 600 °C have caused cracking of the thin YSZ film, and a more serious damages to the YSZ film at 700 °C might occur than those at the other temperatures.

3.3. Reduction of reoxidized Ni/YSZ anodes

All the anodes were reduced again with a blending gas of 5% H_2 and 95% He after reoxidation. Fig. 6 shows the variation of the ohmic resistance with reduction time. Except the cell at 700 °C, all the cells show that the ohmic resistance rapidly decreases to stable values within 10 min. This indicates that the nickel conduction network forms much more easily than the NiO conduction network. A larger peak appears on the ohmic resistance curve of 700 °C, which reflects a larger fluctuation of ohmic resistance. The peak should be related to oxygen leaking from the cathode to the anode due to YSZ film fractures.

Fig. 7 shows the variation of open circuit potential during the reduction of the reoxidized anode. For most cells, the open circuit potentials increase rapidly which are concurrent with the variation of ohmic resistance with reduction time. All the cells, which were previously reoxidized at above 600 °C, exhibit a final OCV much lower than the ideal value, especially for the cell reoxidized 700 °C. This depicts that the electrolyte films in these cells have cracked during reoxidation. The cell which was previously reoxidized at 500 °C gives the best OCV after the re-reduction, consistent with the small change of ohmic resistance in the reoxidation process. The higher temperature reoxidation usually causes a larger anode volume expansion, which could severely damage the integrity of the YSZ film. On the other hand, it was found from the dilatometer measurements that the anode volume expansion was sensitive to minor variations in the anode microstructure, which originated from either the preparation or the nickel reorganization during the initial reduction [15]. This is probably the reason that reoxidation at 700 °C has produced the most severe damage to the YSZ film although these cells are from the same batch.

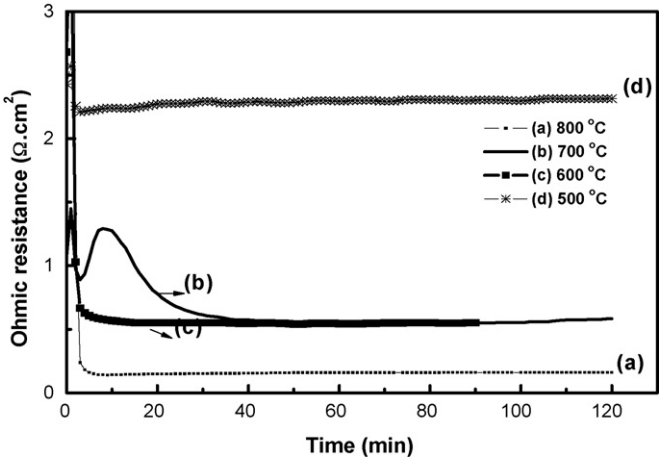

Fig. 6. Variation of cell ohmic resistance with reduction time at (a) 800 °C, (b) 700 °C, (c) 600 °C and (d) 500 °C.

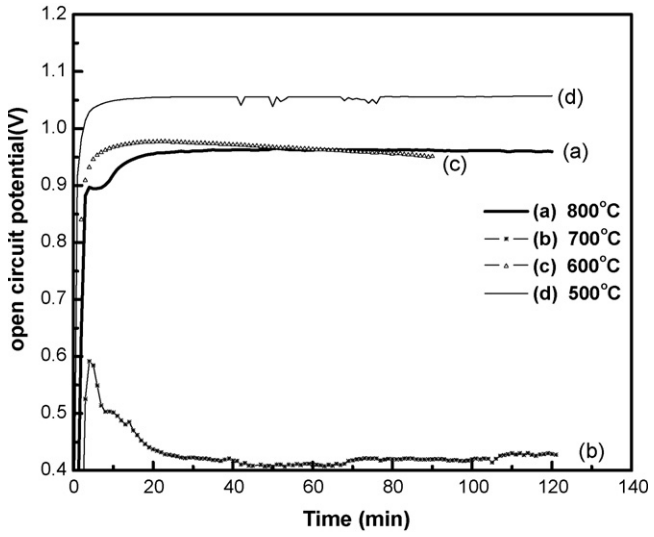

Fig. 7. Variation of open circuit potential with reduction time at (a) 800 °C, (b) 700 °C, (c) 600 °C and (d) 500 °C.

4. Conclusions

The redox behaviour of a Ni–YSZ anode in cells has been investigated through the monitoring of ohmic resistance using electrochemical impedance spectroscopy and the open circuit voltage. Anode reoxidation can be divided into three stages: an initial stage with a slow increase of ohmic resistance, a quick oxidation stage with a sharp increase of ohmic resistance and the last stage with a slight decrease of ohmic resistance. The OCV curves indicate that cell cracking has occurred in the quick oxidation stage. The cell with an anode reduced at 800 °C could only bear the reoxidation below 500 °C.

Acknowledgements

The authors gratefully acknowledge the financial support from the Ministry of Science and Technology of China (Grant nos. 2004CB719506 and 2005CB221404).

References

[1] S. DeSouza,.S.J. Visco, L.C. De Jonghe, Solid State Ionics 98 (1997) 57–61.
[2] Y. Jiang, A.V. Virkar, J. Electrochem. Soc. 150 (7) (2003) A942–A951.
[3] Y.J. Leng, S.H. Chan, K.A. Khor, S.P. Jiang, Int. J. Hydrogen Energy 29 (2004) 1025–1033.
[4] R.N. Basu, G. Blass, H.P. Buchkremer, D. Stöver, F. Tietz, E. Wessel, I.C. Vinke, J. Eur. Ceram. Soc. 25 (4) (2005) 463–471.
[5] M. Cassidy, G. Lindsay, K. Kendall, J. Power Sources 61 (1996) 189–192.
[6] D. Fouquet, A.C. Müller, A. Weber, E. Ivers-Tiffée, Ionics 8 (2003) 103–108.
[7] D. Waldbillig, A. Wood, D.G. Ivey, Solid State Ionics 176 (2005) 847–859.
[8] D. Waldbillig, A. Wood, D.G. Ivey, J. Power Sources 145 (2) (2005) 206–215.
[9] J. Malzbender, E. Wessel, R. Steinbrech, Solid State Ionics 176 (29–30) (2005) 2201–2203.
[10] O.H. Kwon, G.M. Choi, Solid State Ionics 177 (2006) 3057–3062.
[11] Y. Zhang, B. Liu, B. Tu, Y. Dong, M. Cheng, Solid State Ionics 176 (29–30) (2005) 2193–2199.
[12] D.W. Dees, T.D. Claar, T.E. Easler, D.C. Fee, F.C. Mrazek, J. Electrochem. Soc. 134 (1987) 2141–2146.
[13] J.-H. Lee, H. Moon, H.-W. Lee, et al., Solid State Ionics 148 (2002) 15–26.
[14] T. Klemensø, C.C. Appel, M. Mogensen, Electrochem. Solid State Lett. 9 (9) (2006) A403–A407.
[15] T. Klemensø, C. Chung, P.H. Larsen, M. Mogensen, J. Electrochem. Soc. 152 (11) (2005) A2186–A2192.